Title	Vertical orientation with a narrow distribution of helical peptides immobilized on a quartz substrate by stereocomplex formation
Author(s)	Nakayama, Hidenori; Manaka, Takaaki; Iwamoto, Mitsumasa; Kimura, Shunsaku
Citation	Soft Matter (2012), 8(12): 3387-3392
Issue Date	2012-02-14
URL	http://hdl.handle.net/2433/169679
Right	© The Royal Society of Chemistry
Type	Journal Article
Textversion	author

Vertical Orientation with a Narrow Distribution of Helical Peptides Immobilized on Quartz Substrate by Stereocomplex Formation

Hidenori Nakayama[1], *Takaaki Manaka*[2], *Mitsumasa Iwamoto*[2]* *and Shunsaku Kimura*[1]*

1) Department of Material Chemistry, Graduate School of Engineering, Kyoto University, Kyoto-Daigaku-Katsura, Nishikyo-ku, Kyoto 615-8510, Japan

2) Department of Physical Electronics, Tokyo Institute of Technology, 2-12-1 O-okayama, Meguro-ku, Tokyo 152-8552, Japan

E-mail: iwamoto.m.ac@m.titech.ac.jp; shun@scl.kyoto-u.ac.jp

Table of contents entry

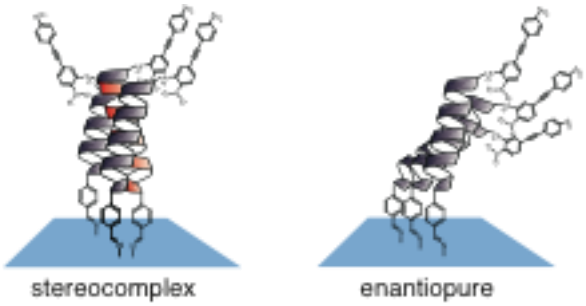

Stereocomplex helical peptides self-assembled into monolayers of more vertical orientation with a narrower distribution than enantiopure peptides based on second-harmonic generation studies.

Abstract

Second-harmonic generation (SHG) of a donor–π–acceptor (D–π–A) chromophore attached to helical peptides was used for evaluation of self-assembled monolayer structure of a stereocomplex of helical peptides. A stereocomplex SAM of a left-handed helical conjugate (**D17**) and a right-handed helical one (**L17**) showed four times larger SHG intensity than a stereocomplex SAM of a left-handed helical **D17** and a right-handed helical peptide without the D–π–A chromophore (**LA16**), which agrees well with dependence of SHG intensities on the surface

densities of the D–π–A chromophore. The SHG intensities of enantiopure SAMs of **D17** and **L17** are, however, 47% and 27% of that of a stereocomplex SAM of **D17** and **L17,** respectively. These differences can be explained only after taking a larger distribution of the tilt angle of the chromophore in the enantiopure SAMs than in the stereocomplex SAM of **D17** and **L17**. On the basis of these analyses, it is concluded that a stereocomplex SAM of a left-handed helix and a right-handed helix constitutes a well-ordered structure, where the tilt angle of the helical peptide from the surface normal becomes small with a narrow distribution due to stereocomplex formation.

1. Introduction

Helical peptides have been reported to form densely packed self-assembled monolayers (SAMs) with vertical orientation on gold surface.[1-11] Most of the helical peptide-SAMs fabricated so far were generally prepared by using a right-handed helix. Recently Ueda et al. showed that a mixture of a right-handed helix and a left-handed helix formed a sheet self-assembly in a buffer solution, where a right-handed helix and a left-handed helix were aligned side-by-side with perpendicular orientation against the sheet surface. Electron diffraction from the sheet clearly showed the helices took a crystalline structure of a square lattice due to stereocomplex formation.[12,13] This finding prompted us to prepare a helix-SAM with using a mixture of a right-handed helix and a left-handed helix.

Usually helix-SAMs are characterized by molecular tilt angles from the surface normal, which are analyzed by FTIR reflection absorption spectroscopy (RAS).[14-17] However, the tilt angle obtained from RAS reflects the average value of the SAM with no information on distribution of the tilt angle. In this article, in order to obtain deeper insights on the molecular alignment in the helix-SAMs, we adopted second-harmonic generation (SHG) as a main characterization technique. Since SHG is surface specific, it has rapidly developed to be a major measurement technique for

characterizing organic layers.[18,19] Owing to some formulas on relationship between the molecular orientation in a membrane and SHG intensity, we can now precisely determine the orientation with its distribution. Taking assumptions of $C_{\infty v}$ and predominant hyperpolarizability of $\beta_{z'z'z'}$ about a chromophore in a SAM, non-vanishing components of second-order sensitivity of a SAM χ are related with $\beta_{z'z'z'}$ as eqs (1) and (2),

$$\chi_{zzz} = N_s \langle \cos^3\theta \rangle \beta_{z'z'z'} \tag{1}$$

$$\chi_{zxx} = \chi_{zyy} = \chi_{xzx} = \chi_{yyz} = \frac{1}{2} N_s \langle \cos\theta - \cos^3\theta \rangle \beta_{z'z'z'} \tag{2}$$

where N_s and θ represent surface density and tilt angle from surface normal, respectively. χ components depend on mean values of $\cos^3\theta$ and $\cos\theta$, suggesting that information on distribution of θ can be obtained by SHG measurements.

We designed compounds **L17** and **D17** (Figure 1). These compounds are linear conjugates of a D–π–A moiety with a high β value and a helical peptide. The D–π–A moiety is a diphenylacetylene having a diethylamine group as an electron donor and a nitro group as an electron acceptor at the both ends. The $\beta_{z'z'z'}$ is the component along the direction of the long axis. The peptide moiety is composed of 17 amino acids. Alternating sequence of D-alanine (D-Ala) and α-aminoisobutyric acid (Aib) was adopted for **D17**. L-Alanine (L-Ala) instead of D-Ala was used for **L17**. This sequence is known to take a stable α-helical structure, which is essential for formation of well-packed and oriented SAMs. The D–π–A moiety was connected on the C-terminal of the peptide moiety through amide linkage at the *ortho* position of the diethylamino group. *p*-Formylbenzoic acid was introduced at the N-terminal of the peptide moiety as a linker to the fused quartz substrate covered with 3-aminopropyl trimethoxysilane. Right- and left-handed helical peptides without the D–π–A moiety, **LA16** and **DA16**, respectively, are also synthesized. Five types of SAMs, **D17/L17**-SAM, **D17**-SAM, **L17**-SAM, **D17/LA16**-SAM, and

L17/DA16-SAM were prepared on fused quartz substrates. On the basis of analysis of SHG from these SAMs, structural differences (molecular density, θ, and distribution of θ) of their SAMs are discussed.

2. Experimental

Materials. D17 and **L17** were synthesized according to Scheme S1 (see the supporting information) according to the conventional liquid-phase method. The purity of the final products was confirmed by HPLC (COSMOSIL $5C^{18}$-AR-300 for **D17** and **L17**, and COSMOSIL Cholester for **DA16** and **LA16**). The D–π–A moiety was synthesized by the Sonogashira coupling. Tetrahydrofuran was used after distillation over calcium hydrate. The other reagents were used as purchased. All products were identified by ^{1}H NMR spectroscopy (Bruker DPX-400). ^{1}H NMR peaks were assigned by HH-COSY spectroscopy. Some of the products were further confirmed by electron ionization (EI) or fast atom bombardment (FAB) mass spectrometry using 3-nitrobenzylaclochol (NBA) as a matrix (JEOL JMS-MS700 for EI, JEOL JMS-HX110A for FAB). The final products were further characterized by high resolution (HR) mass spectrometry.

Preparation of self-assembled monolayer. Five types of SAMs (**D17/L17**-SAM, **D17**-SAM, **L17**-SAM, **D17/LA16**-SAM, and **L17/DA16**-SAM) were prepared by the following procedures: (1) Fused quartz substrates (12 × 40 × 1 mm) were washed with a mixture of 28% aqueous solution of ammonia, 30% aqueous solution of hydrogen peroxide, and water (1/1/5, v/v/v) at 70 °C for 30 min. The substrates were then rinsed with water; (2) The substrates were immersed in a 1 wt % toluene solution of 3-aminopropyl triethoxysilane at 60 °C for 10 min and immediately rinsed successively with toluene, a mixture of toluene and methanol (1/1, v/v), and methanol, followed by nitrogen blow for drying; (3) The coated substrates were immersed in a 0.1 mM

1,2-dichloroethane solution of **D17** or **L17** for preparation of **D17**-SAM or **L17**-SAM, respectively, for 24 hr at 70 °C. For **D17**/**L17**-SAM, a 1,2-dichloroethane solution of a mixture of **D17** and **L17** (0.1 mM for each) were used for immersion. **L17**/**DA16**-SAM and **D17**/**LA16**-SAM were similarly prepared with using the corresponding solutions. After immersion, the substrates were washed with methanol and dried with nitrogen blow.

Optical measurements. Circular dichroism (CD) spectra were measured by a JASCO J-600 CD spectropolarimeter with optical cells of 0.1 and 1 cm optical path length. Absorption spectra of solutions were recorded on a Shimadzu UV-2450PC spectrometer with an optical cell of 1 cm optical path length.

Second harmonic generation measurements: For the SHG measurements, *s*- or *p*-polarized fundamental light was focused on the sample with an incident angle of 45°, using a convex lens (*f* = 100 mm) after passing through an SH-cut filter to eliminate the SHG light from the various optical components. The *p*-polarized SHG light generated at the sample was filtered by a fundamental cut filter to remove intense fundamental light and was detected by a photomultiplier tube (Hamamatsu photonics: R7154) after passing though a monochromator (Shimadzu: SP-120). The signals were averaged by a Boxcar integrator (Stanford Research: SR-250). A light source ranging from 560 nm to 660 nm (0.92 eV) was obtained using an optical parametric oscillator (OPO: Continuum Surelite OPO) pumped by the third-harmonic light of a *Q*-switched Nd-YAG laser (Continuum: SureliteII-10)

3. Results and Discussion

UV and CD spectroscopy. Absorption spectra of **D1**7 and **L17** were recorded in a methanol solution (Figure 2). The two spectra are completely identical to each other. Two of the three bands at 352 and 246 nm are absorption bands mainly from the D–π–A moiety, whereas the other one at

204 nm is assigned to the π–π* transition band of the peptide moiety.[20,21] The molecular extinction coefficients of the three bands are 1.8×10^4, 3.4×10^4, and 7.7×10^4, respectively.

CD spectra of **D1**7 and **L17** are shown in Figure 3. The peptide moiety (Figure 3 left) of **L17** shows two peaks of negative Cotton effects at 208 and 224 nm, which are typical for a right-handed α-helical structure.[22,23] The molar ellipticity of the peak was ca. 2.0×10^4, which is agreeable with those of $(Ala\text{-}Aib)_8$ and $(Leu\text{-}Aib)_8$ reported previously.[24,25] The spectrum of **D17** is a mirror image exactly of that of **L17** as expected, showing that **D17** takes a left-handed α-helical structure.

Induced Cotton effect of the D–π–A moiety is observed around 350 nm (Figure 3 right). In the spectrum of **L17**, a negative broad peak at 350 nm and a positive sharp peak at 260 nm appear. The spectrum of **D17** around 350 nm is also the mirror image of that of **L17**. Time dependent-density functional theory (TD-DFT) calculations support that the induced Cotton effect originates from a twist in the D–π–A moiety (see Supporting Information for details).

Preparation of SAMs. The peptide SAMs were prepared on fused quartz substrates via Shiff-base formation between amino groups of 3-aminopropyl triethoxysilane layer on the fused quartz substrates and formyl groups of the N-terminal of the peptides. Concentrations of peptides in a 1,2-dichloromethane solution is critical for the quality of the SAMs. When the concentrations are too high, SAMs are covered by physisorbed molecules as well. We checked SHG from **D17**-SAM and **L17**-SAM prepared from 0.5 and 0.1 mM solutions, which showed reasonable SHG intensities. The condition of 0.1 mM solution is thus adopted.

Second-order susceptibility of the D–π–A moiety. The SHG intensities from the **D17/L17**-SAM and Y-cut quartz as a function of the light incident angle ϕ_{in} ($-30 < \phi_{in} < 30$) were recorded under the *p–p* setup (Figure 4). The wavelength of the incident light was 560 nm. Maker fringes were not clearly observed for the both samples because of insufficient monochrome laser

light and out of focus on the samples.

The relative SHG light intensity from the SAM against the Y-cut quartz in the *p*–*p* set up, $I_r(2\omega)^{p-p}$, is expressed as eq.(3),

$$I_r(2\omega)^{p-p} = \frac{1}{(\chi_q d_q)^2}\left|(A_{zzz}\chi_{zzz} + A_{xzx}\chi_{xzx} + A_{zxx}\chi_{zxx})\right|^2 \quad (3)$$

where $A_{zzz} = \sin\phi_{out}\sin^2\phi_{in}$, $A_{xzx} = \cos\phi_{out}\sin\phi_{in}\cos\phi_{in}$, $A_{zxx} = \sin\phi_{out}\cos^2\phi_{in}$, $n_{air}\sin\phi_{in} = n_{silica}\sin\phi_{out}$, $n_{air} = 1$, $n_{silica} = 1.5$, χ_q is the second-order susceptibility of the Y-cut quartz (=0.6 pm/V), and d_q is the thickness of the Y-cut quartz (20 μm). Note that the Fresnel factors are excluded in the all three *A* components since they have little contribution. Assuming normal distribution having a standard deviation (SD, σ) of 0.2 rad (12°), 41° of a mean value of the tilt angle θ, and $N_s = 8.4 \times 10^{17}$ m^{-2} (14×10^{17} mol/cm^{-2}),[1] $\beta_{z'z'z'}$ is calculated to be 1.3×10^{-37} m^4/V (= 3.0×10^{-28} esu), which is in the range of typical values for the D–π–A compounds ($1–5 \times 10^{-28}$ esu).[26,27]

Relative intensity of the SHG signal. SHG intensities of all the SAMs were recorded under the *p*–*p* setup ($I(2\omega)^{p-p}$, Table 1). The wavelength and angle of the incident light were 660 nm and 45°, respectively. The SHG intensities of the SAMs are sufficiently larger than that of the quartz substrate treated by 3-aminopropyl triethoxysilane at this wavelength. When the SH intensities are compared among the stereomixed SAMs of the right-handed helix and the left-handed helix, the SHG intensity of **D17/L17**-SAM becomes four times larger than those of **D17/LA16**-SAM and **L17/DA16**-SAM, where the latter two SAMs are an equimolar mixture of the helical peptides with the D–π–A chromophore and without. This observation is understandable since the SHG intensity is related with square of the surface density of the SHG chromophore N_s according to the eqs (1)–(3).[28-30] At the same time, the SAM structures of the tilt angle and its distribution of the SHG chromophore are considered to be similarly reserved among the SAMs composed of a mixture of the right-handed helix and the left-handed helix irrespective of the SHG chromophore

concentration. The scaffolds of the stereomixed right-handed and the left-handed helical peptide SAMs are therefore very effective to align regularly the chromophore attached to the helices.

When the SHG intensity is compared between the enatiopure SAM and the stereomixed SAM, the SHG intensities of **D17**-SAM and **L17**-SAM become about half and one-fourth of that of **D17/L17**-SAM, respectively, despite of the D-π-A chromophore being attached all to the helical peptide in these SAMs. A plausible explanation for the difference is suggested that the surface density of the D–π–A chromophore of the enantiopure SAMs may be smaller than that of the stereomixed **D17/L17**-SAM due to the different tilt angle θ of the D-π-A chromophore. In the present system, the quartz substrate is used, which cannot be subjected to the FT-IR reflection absorption spectroscopy to obtain information of the tilt angle of the helix from the surface normal. On the basis of our experience, however, the tilt angle of helices became smaller with mixing a helical peptide with the opposite helical sense, supporting this explanation.

Another factor contributing to the second-order susceptibility of a SAM can be the local field factor *f*. *f* is generally described by the Lorentz–Lorenz correction, $f = (n^2 + 2)/3$, where *n* is the refractive index at the optical frequency. The correction, however, presumes a crystal structure, which is not the case of the SAMs. We thus omitted this factor in eq. (3).

Molecular orientation and its distribution. SHG measurements were conducted to obtain information on θ and σ using an incident light of 560 nm. Under the assumptions of the $C_{\infty v}$ symmetry of the D–π–A moiety and $\beta_{z'z'z'}$ as the major nonlinear optical molecular polarizability, the ratio of SHG signals can be expressed as

$$\frac{I(2\omega)^{s-p}}{I(2\omega)^{p-p}} = \frac{4\left(\langle\cos\theta\rangle - \langle\cos^3\theta\rangle\right)^2}{5\langle\cos\theta\rangle^2 - 6\langle\cos\theta\rangle\langle\cos^3\theta\rangle + 5\langle\cos^3\theta\rangle^2} \quad (4)$$

where $I(2\omega)^{s-p}$ and $I(2\omega)^{p-p}$ represent the intensities of *p*-polarized SHG light obtained from *s*-polarized incident light and *p*-polarized incident light, respectively.[31] The SHG signal ratios are

thus dependent on θ and its distribution σ. Indeed, Figure 5a shows the calculated curves of eq. (4) with different σ (σ = 0.01–0.5 rad), showing that the ratio monotonically increases as θ increases, and decreases as σ increases. Figure 5b shows calculated SHG intensity of eq. (3) as a function of θ with different σ. (Note that ϕ_{in} = 45°, and the term of $1/(\chi_q d_q)^2$ is omitted for simplicity.) The curves show again the decrease of the SHG intensity with the increase of σ.

Two kinds of experimental values, $I(2\omega)^{p-p}$ and $I(2\omega)^{s-p}/I(2\omega)^{p-p}$, are not enough to determine uniquely the three parameters, θ, σ, and N_s, of the SAMs. We therefore try to find out the self-consistent set of these values with reasonable assumptions. First assumption is to set σ values of 0.2 and 0.5 for the stereomixed and the enantiopure SAMs, respectively. As described before, we found out the stereomixed SAMs were composed of more vertically oriented helices than the enantiopure SAMs, suggesting the smaller θ value and the smaller σ value of the stereomixed SAMs than the enatiopure SAMs. With using the experimental values of $I(2\omega)^{s-p}/I(2\omega)^{p-p}$ and these σ values, θ values were determined from eq. (4) (Table 1). Second assumption is to set the relative values of N_s of 1.0, 0.87, 0.67, 0.5, and 0.5 for **D17/L17**, **D17**, **L17**, **D17/LA16**, and **L17/DA16** SAMs, respectively. These values are in agreeable with the previous interpretation that the stereomixed SAMs should have similar structural parameters of θ and σ, and the helices in the enantiopure SAMs should more tilted with smaller N_s. As listed at the first and sixth rows in Table 1, the experimental result can be well explained by the calculation under these assumptions. On the other hand, when we assume the same σ value of 0.2 for all the SAMs, θ is estimated to be 41° for all the SAMs, and the relative molecular densities should be 0.68 and 0.51 for **D17**-SAM and **L17**-SAM, respectively. However, the density of 0.51 is too sparse to form the helical SAMs with θ of 41°. The stereomixed SAMs therefore should be composed of more vertically oriented helices with smaller θ and σ than those of the enatiopure SAMs, even though the σ values used here do not have quantitative accuracy.

The above conclusion is supported by the observation of the stereomixed helical membrane recently reported by Ueda et al.[12,13] They prepared a sheet-shaped molecular assembly from a mixture of right-handed and left-handed helices in the hydrophobic blocks of amphiphilic peptides. TEM observation clearly showed a square lattice arrangement of the helices in the sheet-shaped membrane, whilst the enantiopure membrane was less ordered. Taken together, a mixture of right-handed and left-handed helices has a strong tendency to form a well ordered structure with stacking side-by-side to be a checkered pattern.

Conclusion

Novel linear conjugates of helical peptides and a D–π–A chromophore, **D17,** and **L17,** were synthesized. SHG measurements of the five kinds of SAMs, **D17/L17**-SAM, **D17**-SAM, **L17**-SAM, **D17/LA16**-SAM, and **L17/DA16**-SAM were carried out. β of the D–π–A moiety in **D17/L17**-SAM is estimated to be 1.3×10^{-37} m^4/V (3.0×10^{-28} esu), which is comparable to the reported values of D–π–A compounds. $I(2\omega)^{p-p}$ values of the enantiopure SAMs were as low as 47% and 27% of that of the **D17/L17**-SAM. Not only the tilt angle θ but also its distribution σ become smaller in the stereomixed SAMs than the enantiopure SAMs. The stereocomplex formation between the right-handed helix and the left-handed helix should be the reason for the regular structure of the stereomixed SAMs.

Acknowledgement

H.N. acknowledges the Research Fellowships of the Japan Society for the Promotion of Science for Young Scientists.

Supporting Information Available.

Synthetic scheme and details; and TD-DFT calculations on the origin of chirality in the D–π–A moieties. These materials are available free of charge via the Internet at http://xxxx.com.

Table 1. Observed and calculated SH intensity of the SAMs.

	D17/L17	**D17**	**L17**	**D17/LA16**	**L17/DA16**
$I(2\omega)^{p-p}$ [a] (relative, experimental)	100	47	27	25	24
$I(2\omega)^{s-p}/I(2\omega)^{p-p}$ (experimental)	0.21	0.23	0.23	0.23	0.23
σ (rad, assumption)	0.2	0.5	0.5	0.2	0.2
$\theta^{(b)}$ (deg, calculation)	41	59	59	41	41
N_s (relative, assumption)	1.0	0.87	0.67	0.5	0.5
$I(2\omega)^{p-p}$ [c] (relative, calculation)	100	47	27	25	25

(a) the value of **D17/L17**-SAM is set to be 100; (b) calculation of eq. (4) (shown in Figure 5a) with the assumption of σ; (c) products of the term $|(A_{zzz}\chi_{zzz} + A_{zzz}\chi_{zzz} + A_{zzz}\chi_{zxx})|^2$ in eq. (3) (shown in Figure 5b) and N_s assumed. Normalized to the value of **D17/L17.**

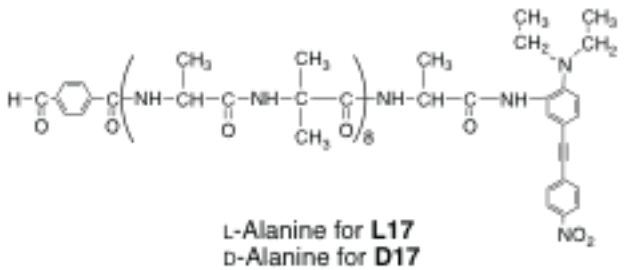

L-Alanine for **L17**
D-Alanine for **D17**

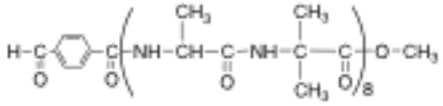

L-Alanine for **LA16**
D-Alanine for **DA16**

Figure 1. Chemical structures of **L17**, **D17**, **LA16**, and **DA16.**

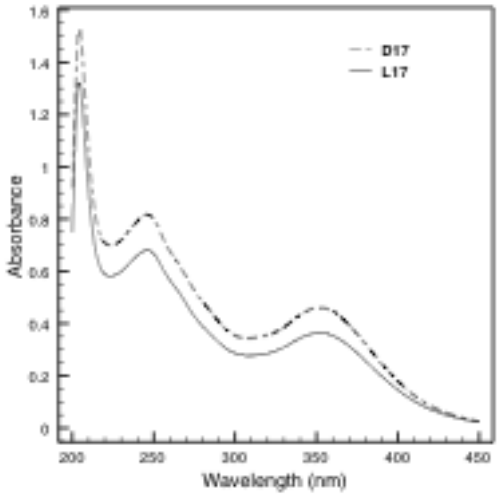

Figure 2. Absorption spectra of **D17** and **L17** in methanol.

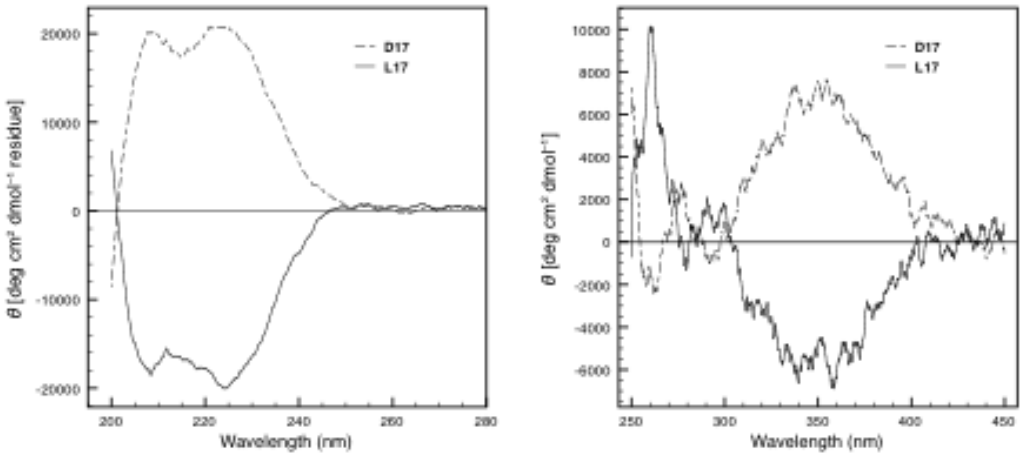

Figure 3. CD spectra of **D17** and **L17** in methanol.

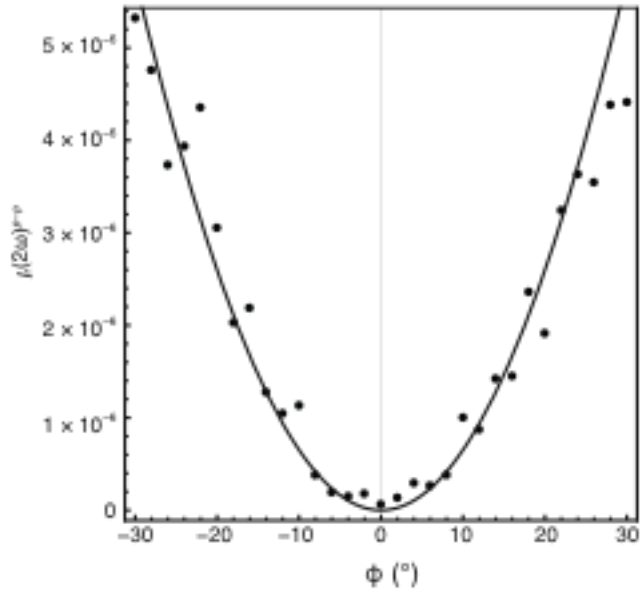

Figure 4. The SHG signals of **D17/L17**-SAM with a fitting line using eq. (3).

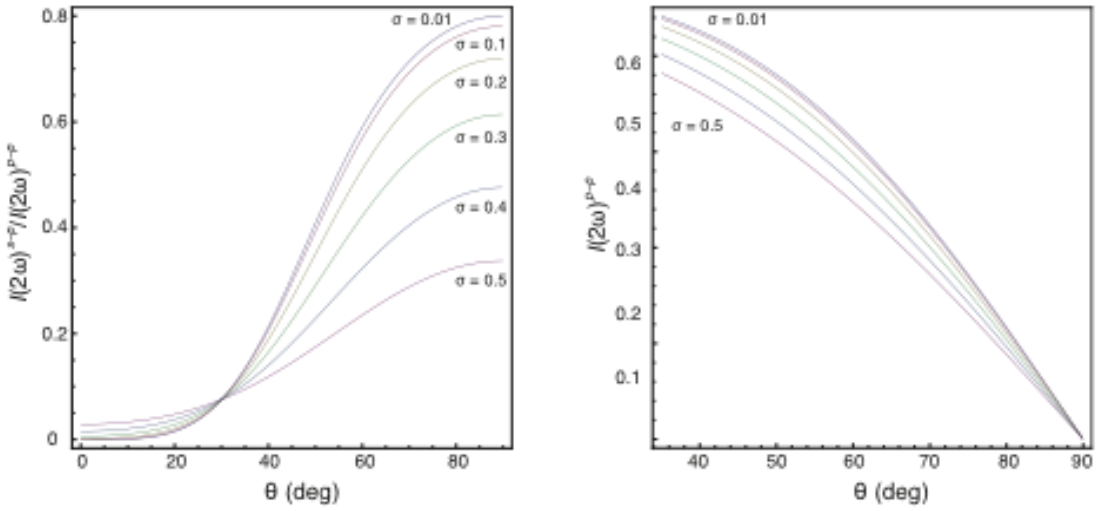

Figure 5. Calculated curves of SHG intensity vs θ assuming the normal distribution of σ = 0.01–0.5 rad in molecular orientation: (a) calculation of eq. (4) and (b) calculation of the term $|(A_{zzz}\chi_{zzz} + A_{zzz}\chi_{zzz} + A_{zzz}\chi_{zxx})|^2$ in eq. (3).

References

1. K. Takeda, T. Morita, and S. Kimura, *J. Phys. Chem. B*, 2008, **112**, 12840-12850.
2. Y. Arikuma, H. Nakayama, T. Morita, and S. Kimura, *Angew. Chem. Int. Ed.*, 2010, **49**, 1800-1804.
3. Y. Arikuma, K. Takeda, T. Morita, M. Ohmae, and S. Kimura, *J. Phys. Chem. B*, 2009, **113**, 6256-6266.
4. M. M. Galka and H. Kraatz, *ChemPhysChem*, 2002, **3**, 356-359.
5. Y. Long, E. Abu-Irhayem, and H. Kraatz, *Chem. Eur. J.*, 2005, **11**, 5186-5194.
6. H. S. Mandal and H. Kraatz, *Chem. Phys.*, 2006, **326**, 246-251.
7. S. Sek, A. Misicka, K. Swiatek, and E. Maicka, *J. Phys. Chem. B*, 2006, **110**, 19671-19677.
8. Y. Arikuma, H. Nakayama, T. Morita, and S. Kimura, *Langmuir*, 2011, **27**, 1530-1535.
9. T. Morita, S. Kimura, S. Kobayashi, and Y. Imanishi, *J. Am. Chem. Soc.*, 2000, **122**, 2850-2859.
10. S. Yasutomi, T. Morita, Y. Imanishi, and S. Kimura, *Science*, 2004, **304**, 1944-1947.
11. T. Morita, K. Yanagisawa, and S. Kimura, *Polym. J*, 2008, **40**, 700-709.
12. M. Ueda, A. Makino, T. Imai, J. Sugiyama, and S. Kimura, *Chem. Commun.*, 2011, **47**, 3204-3206.
13. M. Ueda, A. Makino, T. Imai, J. Sugiyama, and S. Kimura, *Soft Matter*, 2011, **7**, 4143-4146.
14. Y. Miura, S. Kimura, Y. Imanishi, and J. Umemura, *Langmuir*, 1998, **14**, 2761-2767.
15. Y. Miura, S. Kimura, Y. Imanishi, and J. Umemura, *Langmuir*, 1998, **14**, 6935-6940.
16. Y. Miura, S. Kimura, Y. Imanishi, and J. Umemura, *Langmuir*, 1999, **15**, 1155-1160.
17. Y. Miura, G. Xu, S. Kimura, S. Kobayashi, M. Iwamoto, Y. Imanishi, and J. Umemura, *Thin Solid Films*, 2001, **393**, 59-65.
18. R. W. Boyd, *Nonlinear Optics, Third Edition*, Academic Press, 3 ed., 2008.
19. T. Verbiest, K. Clays, and V. Rodriguez, *Second-order Nonlinear Optical Characterization Techniques: An Introduction*, CRC Press, 2009.
20. G. A. Olah and H. W. Huang, *J. Chem. Phys.*, 1988, **89**, 2531.
21. K. A. Bode and J. Applequist, *J. Am. Chem. Soc.*, 1996, **100**, 17825-17834.
22. Y. Chen, J. T. Yang, and H. M. Martinez, *Biochemistry*, 1972, **11**, 4120-4131.
23. G. Holzwarth and P. Doty, *J. Am. Chem. Soc.*, 1965, **87**, 218-228.
24. M. Kai, K. Takeda, T. Morita, and S. Kimura, *J. Pept. Sci.*, 2008, **14**, 192-202.
25. K. Kitagawa, T. Morita, and S. Kimura, *J. Phys. Chem. B*, 2005, **109**, 13906-13911.
26. D. Li, T. J. Marks, and M. A. Ratner, *J. Phys. Chem.*, 1992, **96**, 4325-4336.
27. D. R. Kanis, M. A. Ratner, and T. J. Marks, *Chem. Rev.*, 1994, **94**, 195-242.
28. I. R. Girling, N. A. Cade, P. V. Kolinsky, R. J. Jones, I. R. Peterson, M. M. Ahmad, D. B. Neal, M. C. Petty, G. G. Roberts, and W. J. Feast, *J. Opt. Soc. Am. B*, 1987, **4**, 950-954.
29. S. Yokoyama, T. Nakahama, A. Otomo, and S. Mashiko, *Thin Solid Films*, 1998, **331**, 248-253.
30. G. Decher, B. Tieke, C. Bosshard, and P. Gunter, *J. Chem. Soc., Chem. Commun.*, 1988, 933-934.

31. T. Manaka, D. Taguchi, D. Nakamura, H. Higa, and M. Iwamoto, *Colloids Surf., A*, 2005, **257-258**, 319-323.